Journal of Molecular Catalysis A: Chemical 323 (2010) 33–39

Contents lists available at ScienceDirect

Journal of Molecular Catalysis A: Chemical

journal homepage: www.elsevier.com/locate/molcata

Enhanced catalytic activity of benzene hydrogenation over nickel confined in carbon nanotubes

Hongxiao Yang[a,b], Shaoqing Song[a], Richuan Rao[a], Xizhang Wang[a], Qing Yu[a], Aimin Zhang[a,*]

[a] School of Chemistry and Chemical Engineering, Key Laboratory of Mesoscopic Chemistry of MOE, Nanjing University, Nanjing 210093, PR China
[b] Analysis and Testing Center, Nanjing Normal University, Nanjing 210097, PR China

ARTICLE INFO

Article history:
Received 13 October 2009
Received in revised form 25 February 2010
Accepted 2 March 2010
Available online 9 March 2010

Keywords:
Carbon nanotubes
Nickel
Confinement
Hydrogenation of benzene
Defects

ABSTRACT

6.0 wt.% Ni was filled in the channel or deposited on the outer surface of carbon nanotubes (CNTs) by capillarity or deposition to obtain two kinds of catalysts (denoted as Ni-filled-CNTs and Ni-deposited-CNTs, respectively). The catalysts were characterized by transmission electron microscopy (TEM), X-ray powder diffraction (XRD), nitrogen adsorption–desorption isothermal, thermogravimetric analysis (TGA), H_2-temperature programmed reduction (H_2-TPR), and Raman spectroscopy. The catalytic performance was evaluated by the hydrogenation of benzene to cyclohexane in the gas phase at 160 °C and under atmospheric pressure. The conversion of benzene on the Ni-filled-CNTs catalyst is 4.6 times as that of Ni-deposited-CNTs. The research results indicate that the enhanced catalytic activity can be attributed to the confinement of CNTs with more defects which provides facile reduction, reinforced reactivity and increased reactants concentrations due to larger charge transfer and deficient electron in tubular micro-reactor. And the gaps formed on the sidewall of CNTs during the treatment process also play an important role for decreasing the diffuse resistant kinetically.

1. Introduction

As a novel nanocarbon material, carbon nanotubes (CNTs) possess several unique features, such as excellent graphitized tube-wall, nanometer-sized channel, sp^2-C-constructed surface and large specific surface areas. They also display peculiar electrical conductivity, mechanical strength, high thermal stability, and supernormal capacity for hydrogen storage. In the past decade, CNTs have drawn great attention as a new support material in catalysis, and a lot of research has been reported involving hydrogenation [1], selective hydrogenation [2], hydroformylation [3], selective dehydrogenation [4], ammonia synthesis [5], Fischer–Tropsch synthesis [6], methanol synthesis [7] and higher alcohol synthesis [8]. All of these render this kind of nanostructured carbon materials to be a promising catalyst support whether from a viewpoint of fundamental research or of potentially industrial application [9–12].

Recent results obtained in the laboratory have shown that the active phase inside CNTs exhibited an extremely high activity or selectivity compared to that observed on traditional grain catalysts. In our previous work [13], Pd clusters were introduced into the channel of CNTs and showed higher catalytic activity than Pd clusters upon the traditional support Y zeolite and activated carbon. Bao et al. [14–17] displayed their excellent works and proposed the confinement of CNTs as support. The view of electron-deficient was used to explain the increase of activity. The deformation of sp^2 hybridization in graphitic walls causes π-electron density to shift from the concave surface to the convex surface, leading to an electrical potential difference between inside and outside of CNTs [18,19]. On the other hand it is also considered that the confinement would cause the increase of diffusion resistance during catalysis process [17].

It is known that the CNTs are not perfect and have defects in most situations. The defects can affect the physical properties and chemical behavior of CNTs. Theoretical calculation indicated that the structural defects such as topological defects, vacancies, and chemical modification can introduce new properties of CNTs, expanding the scope of potential applications [20]. The binding energy between CNTs and transition metals was significantly enhanced when defects were introduced into the CNTs [21]. Guo and Kiang show the defect has a crucial function in spontaneously adjusting the internal pressure [22,23]. However there are few researches on the effect of defects on the catalytic performance of encapsulated component inside CNTs.

In the present work, Ni nanoparticles were filled successfully in the inside CNTs by using capillarity, and benzene hydrogenation in gas phase was chosen as probe reaction to explore the promoting of the tubular nanostructural CNTs through comparing to those of Ni

* Corresponding author. Tel.: +86 25 83686235; fax: +86 25 83317761.
E-mail address: zhangam@nju.edu.cn (A. Zhang).

1381-1169/$ – see front matter © 2010 Elsevier B.V. All rights reserved.
doi:10.1016/j.molcata.2010.03.005

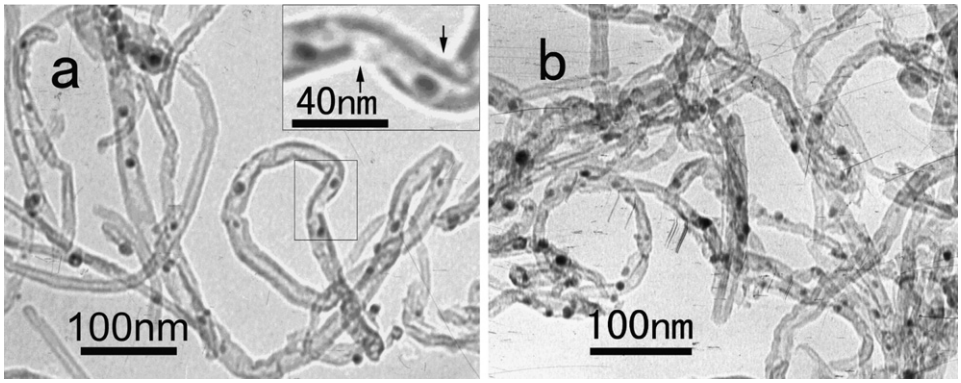

Fig. 1. TEM micrograph of the catalysts. (a) Ni-filled-CNTs (inset shows the amplification of the square part) and (b) Ni-deposited-CNTs.

nanoparticles deposited on the outer surface of CNTs. The reactivity of Ni species within the CNTs, the influence of structural defects on catalytic performance, and the confinement of CNTs have been investigated in detail.

2. Experimental

2.1. Catalyst preparation

Multi-walled CNTs with the outer diameter of 8–20 nm and the inner diameter of 4–8 nm were supplied by Tsinghua Nanfeng nano-power materials limited company. In order to fill the Ni species into the channel of CNTs, they were treated firstly by mechanical ball milling process in a planetary ball milling apparatus at a rotation speed of 180 rpm. Then the shortened CNTs were treated again by nitric acid to open further the ends of CNTs and to remove impurities. Typically, 3.0 g CNTs were suspended in 150 ml of concentrated HNO_3 (68 wt.%) and refluxed at 60 °C for 6 h. After the mixture cooled to room temperature, it was filtered and washed with distilled water until the pH reached 7, then dried at 60 °C for 12 h, to obtain clean opened CNTs. The nickel salt ($Ni(CH_3COO)_2{\cdot}6H_2O$) was dissolved in an appropriate amount of acetic acid, the above opened CNTs, which had been heated previously, were mixed into this solution (the volume ratio of liquid to solid is 1). Owing to the capillary force and temperature difference, nickelous liquid can be sucked into the channel of CNTs easily and a paste-like mixture was obtained. Subsequently it dried slowly at 60 °C for 4 h under vacuum condition. Then the dried matter was calcinated at 450 °C in N_2 for 3 h. Finally obtained catalyst was denoted as Ni-filled-CNTs, and it has been reduced in H_2 flow at 500 °C for 3 h before catalytic reaction.

As compared sample, the same amount of Ni was deposited on the outer surface of CNTs. The pristine CNTs were purified by refluxing in dilute HNO_3 solution (37 wt.%) at 60 °C for 6 h to remove impurities. Then these unopened CNTs were immerged into nickel acetate solution (the volume ratio of liquid to solid is 15), and stirred at 60 °C overnight until they formed pasty mass. Subsequently it was evaporated at 80 °C under atmospheric pressure for 3 h, then gradually heated to 450 °C in N_2 and kept for 3 h. The obtained final sample was denoted as Ni-deposited-CNTs. The catalyst has been reduced in H_2 flow for 3 h at 500 °C before catalytic reaction. In order to compare the effect of support, the same amount of Ni was deposited on activated carbon (AC) which was furnished from Aldrich Chemical Company Inc. The same procedures as Ni-deposited-CNTs were used to prepare the comparing sample Ni-deposited-AC. The Ni-content of all prepared catalysts is 6.0 wt.%.

2.2. Catalyst characterization

TEM observation was carried out on a JEM-200 transmission electron microscope and operated at 200 kV. The samples were ultrasonically dispersed in ethanol and placed onto a carbon film supported on a copper grid. XRD pattern was collected on an X'TRA X-ray diffractometer (ARL, Switzerland) using Cu Kα radiation (λ = 1.5418 Å). Chemical analysis of the samples was analyzed on Leeman Labs Prodigy ICP-AES instrument. Nitrogen adsorption measurements were determined by Micromeritics ASAP 2000 at −196 °C, and the BET surface areas as well as pore size distribution were taken from the isotherms. TG curve was measured by Perkin-Elmer Pyris 1 thermogravimetric analyzer in different gas atmosphere while the temperature was increased from 25 to 800 °C with a rate of 10 °C/min. Thermogravimetry–mass spectrometry (TG–MS) was followed by mass spectrometry by heating the samples in a flowing N_2 stream (30 ml/min) at a rate of 10 °C/min. The signal (m/e) range from 18 to 56 was monitored by an online mass spectrometer (QMS.403C, Netzsch). The reducibility of sample was studied by TPR in a mixture flow of 5 vol.% H_2 in Ar. The temperature change was from room temperature to 720 °C at a rate of 10 °C/min. Raman spectra were recorded with a Raman spectrometer (Invia, Renishaw) using a laser excitation line at 514.5 nm.

2.3. Catalytic reaction test

The hydrogenation of benzene in gas phase was carried out in a U-type quartz micro-reactor under atmospheric pressure. In a typical catalytic run, 50 mg catalyst was activated in situ with H_2 at 500 °C for 1 h. After activation, the temperature was lowered to 160 °C, the benzene vapor saturated at 30 °C was introduced into the micro-reactor by H_2 at a flow rate of 6 ml/min. The reaction products were analyzed online by a gas chromatography equipped with flame ionization detector (FID) using a 3 mm × 3 m stainless steel column packed with Silicon SE-30 at 100 °C.

3. Results and discussion

3.1. Catalysts characterization

3.1.1. Location and size of nanoparticles

Fig. 1 shows the TEM micrographs of as-prepared Ni-filled-CNTs and Ni-deposited-CNTs. It can be seen that in the case of Ni-filled-CNTs, the Ni particles are in the channel of CNTs as shown in Fig. 1a. Statistics shows that there are more than 80% of Ni particles inside CNTs. In fact, most of the ends of CNTs have been opened as a result of the process of mechanical ball milling and concentrated nitric acid treatment. Due to the relatively low surface tension of the sol-

vent used, an equal amount of liquid was sucked almost entirely into channels of CNTs under the capillary force. The TEM micrograph also displays that the size of the Ni particles ranges from 3 to 7 nm for the Ni-filled-CNTs catalyst. For the Ni-deposited-CNTs, Ni particles ranging from 3 to 8 nm are deposited evenly on the outer surface of CNTs as shown in Fig. 1b. Judged from the micrograph there is no significant difference in the particle size between Ni-filled-CNTs and Ni-deposited-CNTs. It is suggested that there are no significantly difference on the particles size between Ni-filled-CNTs and Ni-deposited-CNTs.

3.1.2. Catalyst component

The XRD patterns of Ni-filled-CNTs, Ni-deposited-CNTs and purified CNTs are shown in Fig. 2. The peaks at 26.2°, 44.2°, and 51.4° observed in the three profiles can be indexed as (0 0 2), (1 0 1), (1 0 2) diffractions of graphite (JCPDS 75-1621), respectively. By comparing the intensity of peaks, no apparent difference was observed, which indicates that the graphene sheets of the CNTs supports have not been destroyed after acid treatment and the loading of Ni species. The diffraction peaks at 36.5° and 43.2° in both Ni-filled-CNTs and Ni-deposited-CNTs correspond to NiO (JCPDS 78-0643), suggesting the Ni species in both samples existed steadily in the form of NiO. Chemical analysis displays that the content of Ni in Ni-filled-CNTs and Ni-deposited-CNTs is 5.9% and 6.0%, respectively.

3.1.3. Pore structure and surface property

The adsorption–desorption isotherms of the three samples and their pore size distribution (PSD) are shown in Fig. 3a and b, respectively. All samples exhibits type II adsorption isotherms with clear hysteresis loops at higher relative pressures as classified by IUPAC [24], suggesting a broad distribution of mesopore in the samples. The amount of N_2 adsorbed on the samples at the relative pressures is very small, <0.1, indicating that micropores are insignificant in the samples [25]. The hysteresis loops H3 appeared at higher

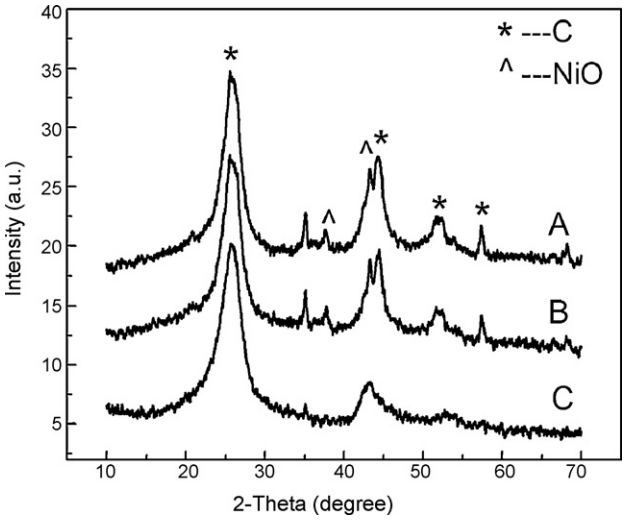

Fig. 2. XRD patterns of sample. (a) Ni-filled-CNTs and (b) Ni-deposited-CNTs, and (C) purified CNTs.

relative pressure are associated with the capillary condensation in mesopores or accumulated pore [25]. Evidently the increase of capillary condensation on Ni-deposited-CNTs is due to increased volume of accumulated pore as shown in Fig. 3b. The deposited nanoparticles are located on the outer surfaces of CNTs, thereby they widen the spaces between the tubes. For the Ni-filled-CNTs catalyst, no distinct difference due to Ni particles was observed when compared to that of purified CNTs, further indicating that Ni particles are located mainly inside CNTs. Table 1 lists the pore properties and BET surface areas of the three samples. The specific surface area of Ni-deposited-CNTs is larger than that of Ni-filled-CNTs, indicating the increased surface areas should be attributed to the increased accumulated pore volume.

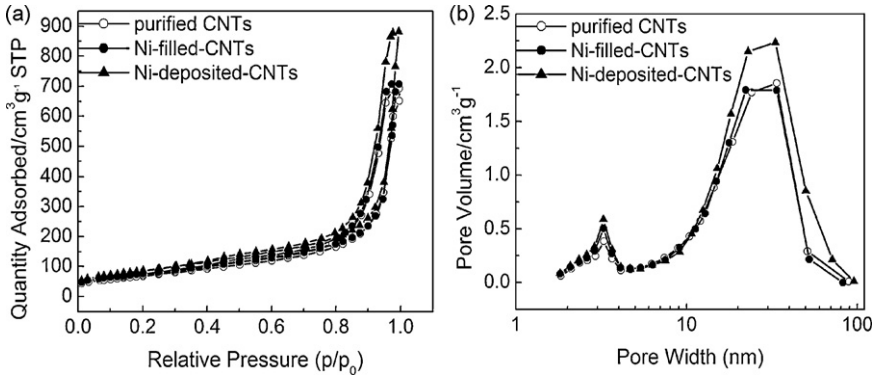

Fig. 3. (a) N_2 adsorption–desorption isotherms and (b) pore size distribution of Ni-filled-CNTs, Ni-deposited-CNTs and purified CNTs.

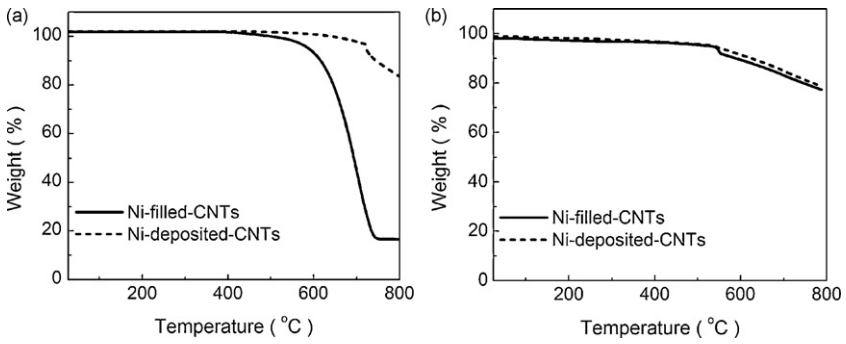

Fig. 4. TG curves of Ni-filled-CNTs, Ni-deposited-CNTs in (a) nitrogen gas flow and (b) argon gas flow.

Table 1
Pore properties and BET surface areas of the different samples.

	Purified CNTs	Ni-filled-CNTs	Ni-deposited-CNTs
BET surface areas	246.6 m^2/g	272.0 m^2/g	307.2 m^2/g
Pore volume	0.8137 cm^3/g	0.8290 cm^3/g	0.8663 cm^3/g

3.1.4. Thermal stability

In order to investigate the thermal stability of both catalysts Ni-filled-CNTs and Ni-deposited-CNTs, the TG measurement was performed in the temperature range of 25–800 °C. It is interesting to note that the TG curves obtained in different inert gases are completely different from each other. The TG curves obtained in N_2 gas (purity 99.95%) are shown in Fig. 4a. The Ni-filled-CNTs was stable up to 500 °C, and then the decomposition starts along with elevated temperature and reaches the maximum at 740 °C, almost complete weight loss is noticed. On the other hand, the Ni-deposited-CNTs catalyst was stable up to 700 °C, its decomposition is slow, and the weight loss is only 16% at 800 °C. However, the weight loss of the two samples is the same when we put them into the atmosphere of Ar gas (purity 99.99%) as shown in Fig. 4b. The weight loss of both samples is only 23% up to 800 °C. To explore the reason for this difference, we repeated the TG experiment using N_2 gas containing different amount of oxygen, and found that there is no difference between Ni-filled-CNTs and Ni-deposited-CNTs, and the TG curve is same as that in air. This indicates the both catalysts have been oxidized at the same degree when the oxygen is sufficient. However the TG curve is different when the carry gas contains trace of oxygen as shown in Fig. 4a. An attached MS analysis shows that the decomposition product of Ni-filled-CNTs is mainly CO_2. Furthermore, the TG–MS experiment under an improved condition (purity of N_2 gas is 99.999% and equipped a deoxidizer) was carried out. It is found that the weight loss of Ni-filled-CNTs is only 3.5% at 800 °C and the decomposition product of Ni-filled-CNTs still is CO_2. It is obvious that the carbon reacts with a small quantity of oxygen-containing groups existed the surface of CNTs. The above experimental results indicated that the CNTs can react with trace of oxygen when they are filled with Ni species.

The enhanced material density in CNTs has been used to explain the phenomena of photoinduced oxidation and sensitivity to the laser irradiation [26,27]. In our research the CNTs are found to be extremely sensitive to trace level of oxygen when they were filled with metal component. It may be interpreted that the transition metal, as the catalyst, accelerates the oxidation of the CNTs because the activation energy for oxidation can decrease considerably after filling [28]. The trace of O_2 may come from the impurity in carrier gas or oxygen-containing groups [29]. In addition, the increased structural defect is also a factor which causes the thermal stability decline [27,28].

3.2. Benzene hydrogenation performance

The conversion of benzene hydrogenation to cyclohexane as a function of time over the three kinds of catalysts (Ni-filled-CNTs, Ni-deposited-CNTs, and Ni-deposited-AC) is represented in Fig. 5a. In all experiments, the product of benzene hydrogenation is only cyclohexane, and the selectivity is 100%. It can be seen that the catalytic activity of Ni supported by CNTs is higher than that of the Ni supported by AC whether it is filled inside or deposited on the outside of CNTs. The steady benzene conversion of the Ni-filled-CNTs and the Ni-deposited-CNTs is 60% and 13%, and turnover of frequency (TOF) value is 2.12 and 0.46 h^{-1}, respectively. The catalytic activity of Ni-filled-CNTs is 4.6 times as that of Ni-deposited-CNTs. It is obvious that the catalytic activity of the Ni-filled-CNTs is much higher than that of the Ni-deposited-CNTs. For the Ni-deposited-AC, the steady benzene conversion and TOF value is only 6% and 0.21 h^{-1}, respectively. No catalytic activity was detected on the purified CNTs (without loading Ni), indicating the catalytic activity comes from Ni species.

To gain insight into the effect of reduction on catalytic performance, we detected the conversion of benzene on the unreduced catalysts which has been activated only in N_2 for 3 h. The reaction condition is the same as that of reduced catalysts, and the conversion of benzene hydrogenation as a function of time is shown in Fig. 5b. It can be seen that for the unreduced Ni-deposited-CNTs catalyst, there is no distinct change compared to reduced catalyst, and steady conversion remains at around 13%. However, for the unreduced Ni-filled-CNTs the conversion curve of benzene is different from that of reduced catalyst. At the beginning of reaction, nearly no activity was detected, until the reaction processed for 1.5 h the conversion of benzene achieves the highest (about 34%). Then the steady conversion remained at around 28%. The result indicates that the Ni inside the tubes also exhibits higher catalytic activity (2.2 times) than those on the outer surface of CNTs despite the incomplete reduction of the Ni species in tubes due to the increased diffusion resistance [17]. Meanwhile it indicates that the H_2 in reactants current is sufficient to make the unreduced catalysts reduce into activated metal component. Reduction or not, it had no significant effect on the Ni species located on the outside of CNTs thanks to the spontaneous reduction action of CNTs, but it influences the Ni species inside CNTs due to the increased diffusion resistance. Besides, for the unreduced Ni-deposited-AC the steady conversion maintained at about 2.0%, which is less than that of reduced Ni-deposited-AC (6.0%), indicating the support AC has no spontaneous reduction action for transition metal oxide.

It is noticeable that there was an induction period at the beginning of reaction for the Ni-filled-CNTs whether it is reduced or not. As shown in Fig. 5a, at the initial stage of reaction, the conversion of benzene increases gradually and reaches a maximum in

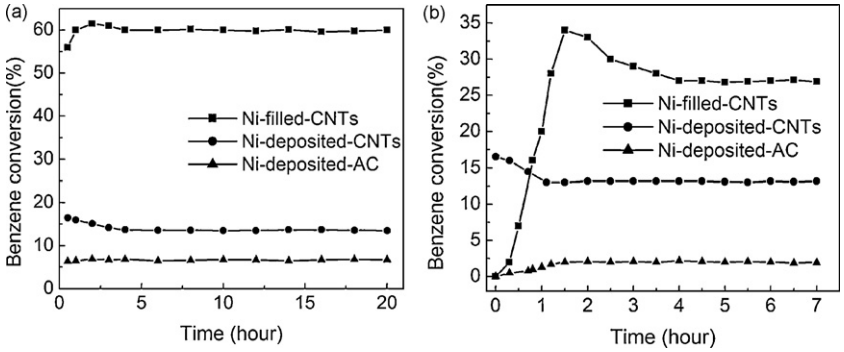

Fig. 5. Conversion of benzene hydrogenation to cyclohexane as a function of time on different catalysts: (a) reduced catalyst by H_2 and (b) unreduced catalysts. Measurements were performed using a mixture of $H_2/C_6H_6 = 4.8$ and a flow of 6 ml min^{-1} at 160 °C and atmospheric pressure.

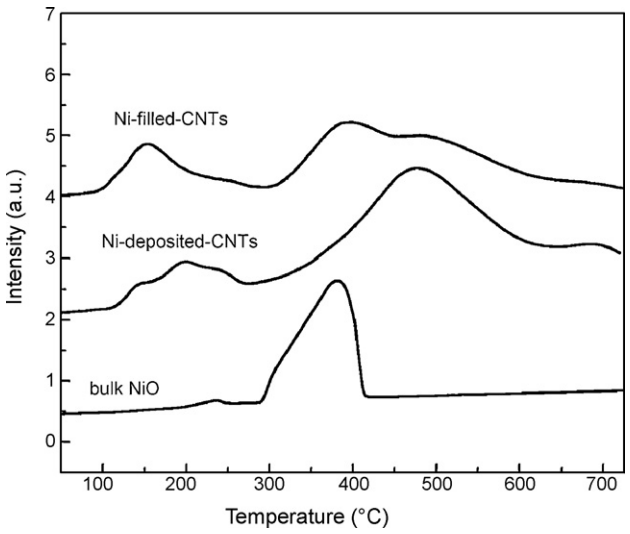

Fig. 6. H_2-TPR profiles of Ni-filled-CNTs, Ni-deposited-CNTs and bulk NiO.

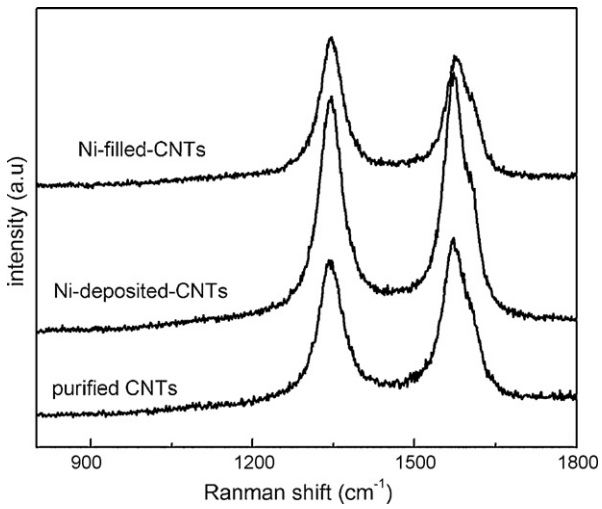

Fig. 7. Raman spectra of Ni-filled-CNTs, Ni-deposited-CNTs and purified CNTs.

2 h, then the rate falls slowly to a steady value (60%) and maintains the conversion for a long time. The induction period also appears on the unreduced Ni-filled-CNTs as shown in Fig. 5b. From it we can see that the conversion of benzene rises rapidly along with the reduction of catalyst by H_2. Actually there is a pressure difference between the inside and outside of CNTs due to the larger entropy of molecules [30,31] and the Bose–Einstein condensation in the interior of CNTs [32,33]. Relative to the conversion decrease which appeared at the beginning of reaction on Ni-deposited-CNTs, the induction period would be a process of overcoming the diffuse resistance, increasing concentration of reactants in the tubular reactor and establishing equilibrium.

3.3. *Effect of CNTs as support on catalytic performance*

The above-mentioned section clearly shows that the catalytic activity of Ni-filled-CNTs is much higher than that of Ni-deposited-CNTs for the hydrogenation of benzene despite the incomplete reduction of the Ni species in tubes. The TEM and BET measurements of catalysts also display that they have the same particles size and similar specific surface areas, the unique difference is the position of Ni species situated in CNTs, suggesting the confinement of CNTs channel can dramatically change the efficiency of a catalyst.

3.3.1. *Reducibility of Ni species in CNTs*

The reducibility of Ni species supported CNTs is a crucial factor influencing its catalytic property. H_2-TPR profiles of the Ni-filled-CNTs, Ni-deposited-CNTs, and compared sample bulk NiO, which is obtained by calcining nickel acetate at 450 °C, are shown in Fig. 6. It can be seen that there are mainly two H_2 consumption peaks at the temperature range of 100–600 °C for the former two catalysts. The first peak may be assigned to the reduction of high-dispersed NiO particles, and the second one assigned to the reduction of the carbon support, since supported transition metal may act as catalyst for the formation of methane via a reaction of hydrogen with the CNTs at higher temperature [34,35]. By comparing to the reduction peak of bulk NiO at around 395 °C, it is found that the reduction temperature of NiO decreased considerably due to the fact that it is supported by CNTs, and for the Ni-filled-CNTs the H_2 consumption temperature is lower than that of Ni-deposited-CNTs, indicating the Ni species inside CNTs can be reduced more easily.

The decrease of reduction temperature of CNTs when filled with metal oxides can be explained by the theory of electron-deficient interior surface of CNTs [18,19]. In the hollow concave surface of CNTs, the strengthened interaction between the electron-deficient concave surface and the anionic oxygen in NiO leads to weak the bonding strength of Ni–O, thereby the reducibility of the Ni species inside CNTs is higher than the Ni species outside CNTs.

3.3.2. *Effect of the structure defects*

Raman spectroscopy was employed to analyze the degree of graphitization of prepared CNTs catalysts. Fig. 7 shows the Raman spectra of Ni-filled-CNTs, Ni-deposited-CNTs and purified CNTs. Two prime intense Raman bands, G-band at 1595.9 cm^{-1} and D-band at 1340.9 cm^{-1}, were detected in the three samples. The G-band can be attributed to the C–C stretching (E_{2g}) mode for the graphite, i.e. characteristic feature of ordered graphite carbon. The D-band is related to the defects and disorders of structures in carbon materials [36]. The intensity ratio (I_D/I_G) of the D- and G-band represents the degree of disorder in graphite layer. It was noted that the I_D/I_G ratio of both purified CNTs and Ni-deposited-CNTs is <1.0 (0.83 and 0.88), indicating good crystallinity of the graphite sheets. However the I_D/I_G ratio of Ni-filled-CNTs increases to 1.16, suggesting the higher level of defects or disorder structure in the case of Ni species filled in channel of CNTs. These disordered carbon walls could be the results of the violent impact of mechanical ball milling and the concentrated acid action of acid treatment process. On the other hand, it was also due to the fact that the transition metal filled CNTs as the catalyst accelerated the decomposition of partial defected carbon sidewall [27], which resulted in forming larger gaps. The phenomena even could be observed by TEM micrograph as shown in the inset of Fig. 1a. It is noticed specially that these gaps often formed on the inflexed sites (showed by arrows) of CNTs, herein the sidewall of CNTs was easily damaged by external force because there are more defects in the inflexed site. Subsequently the nearby Ni particles catalyzed the cracked wall to decompose, thereby formed the broad gaps during the treatment at elevated temperature.

Some research confirmed that the structure defect of CNTs is an important influencing factor on catalytic activity due to the large charge transfer and deficient electron on the defective CNTs compared to that on the defect free CNTs [21]. In fact, as described above, the Ni-filled-CNTs catalyst with more structure defects causes more changes in the reducibility, thermal stability, and sensitivity of reaction. This is due to the large charge transfer from metals to defective CNTs along the nanotube wall, which accelerated the redox inside CNTs [32]. In addition, the substance filled in defected CNTs can escape through defected sites [23,37], suggesting the defected sites

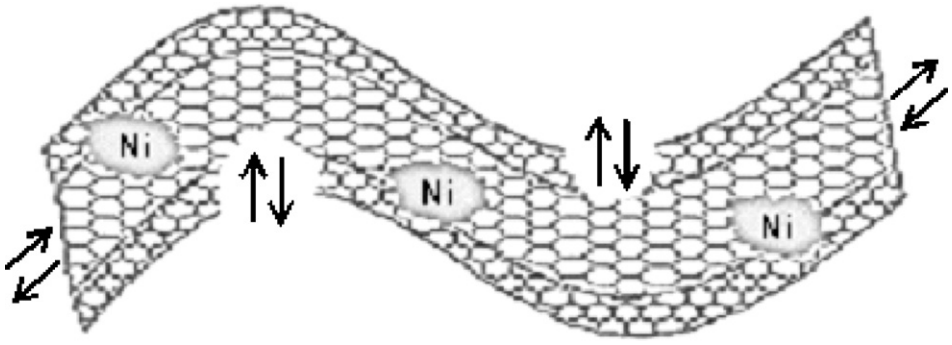

Scheme 1. Schematic diagram for the catalytic hydrogenation of benzene over Ni-filled-CNTs.

can be regarded as the pathway of reactant or product during the catalytic process.

3.3.3. Hydrogenation reaction in micro-reactor

According to the above discussion, a schematic diagram for the catalytic hydrogenation of benzene over Ni-filled-CNTs was proposed as shown in Scheme 1. We can regard the multi-wall CNTs support as a tubular micro-reactor, when the Ni-filled-CNTs is placed in the hydrogen gas containing benzene, the density of hydrogen and benzene inside the tube is higher than the density outside the tube due to the pressure difference between the inside and the outside of CNTs [33]. In the environment of higher pressure of hydrogen, the NiO can be reduced to metallic Ni more easily due to the spontaneous reduction of CNTs with defects. At the same time the reactant molecules have a much more chances to contact with the activated Ni nanopaticle. The hydrogen molecule absorbed by the Ni catalyst dissociates into atomic hydrogen and attack the double-bond of benzene to form cyclohexane. On account of the self-diffusion action along the nanotube axis in tubular micro-reactor [38], the product cyclohexane molecule can desorb from catalyst and diffuse off rapidly. If we compare the end of CNTs to a door, then those gaps can be seen as windows (as shown by arrows in Scheme 1). These windows provide convenient pathways for reactant molecules into and product molecules out, hence reduce the diffuse resistance kinetically and accelerate the conversion of benzene to cyclohexane.

In one word, the effect of CNTs as support on the hydrogenation of benzene would include these factors: increasing the concentration of reactants, facilitating reduction, reinforcing the reactivity, and increasing the diffusion resistance. However the diffusion resistance has been reduced greatly due to gaps created during treatments. Therefore the Ni-filled-CNTs exhibited much higher catalytic activity than the Ni-deposited-CNTs although they are loaded with same amount and particle size of Ni species.

4. Conclusion

The catalytic activity of Ni filled inside CNTs is 4.6 times higher than that of Ni deposited outside CNTs in hydrogenation of benzene. TEM micrographs and BET measurements show that the two kinds of catalysts have similar particle size and specific surface areas. H_2-TPR demonstrates that NiO inside CNTs reduces easily. TG analysis indicates that when Ni species are filled inside CNTs, the reactivity increased greatly. Raman spectrum shows that the Ni-filled-CNTs catalyst has more defects than the Ni-deposited-CNTs. The lower initial activity of unreduced Ni-filled-CNTs suggests the effect of diffusion resistance. The induction period which appeared on the Ni-filled-CNTs represents a process of overcoming the diffuse resistance, increasing concentration of reactant molecules in the tubes, and establishing reaction equilibrium. As a tubular micro-reactor, the gaps formed on the inflexed sites of CNTs provide convenient pathways for reactants entry or products out, reduced the diffuse resistance. Therefore the enhanced catalytic activity on the Ni-filled-CNTs may be attributed to the confinement of multi-walled CNTs with more defects due to large charge transfer and deficient electron, as well as the gaps which decrease the diffusion resistance kinetically.

Acknowledgements

This work was financially supported by the National Natural Science Foundation of China (Project No. 20673056), and the Open Analysis Foundation of Nanjing University.

References

[1] J.M. Planeix, N. Coustel, B. Coq, V. Brotons, P.S. Kumbhar, R. Dutartre, P. Geneste, P. Bernier, P.M. Ajayan, J. Am. Chem. Soc. 116 (1994) 7935–7936.
[2] Y. Li, Z.G. Li, R.X. Zhou, J. Mol. Catal. A: Chem. 279 (2008) 140–146.
[3] R. Giordano, P. Serp, P. Kalck, Y. Kihn, J. Schreiber, C. Marhic, J.L. Duvail, Eur. J. Inorg. Chem. 4 (2003) 610–617.
[4] Z.J. Liu, Z.D. Xu, Z.Y. Yuan, D.Y. Lu, W.X. Chen, W.Z. Zhou, Catal. Lett. 72 (3–4) (2001) 203–206.
[5] Z.L. Li, C.H. Liang, Z.C. Feng, P.L. Ying, D.Z. Wang, C. Li, J. Mol. Catal. A: Chem. 211 (2004) 103–109.
[6] E. van Steen, F.F. Prinsloo, Catal. Today 71 (2002) 327–334.
[7] X. Dong, H.B. Zhang, G.D. Lin, Y.Z. Yuan, K.R. Tsai, Catal. Lett. 85 (3–4) (2003) 237–246.
[8] H.B. Zhang, X.L. Liang, X. Dong, H.Y. Li, G.D. Lin, Catal. Surv. Asia 13 (2009) 41–58.
[9] M.J. Ledoux, R. Vieira, C. Pham-Huu, N. Keller, J. Catal. 216 (2003) 333–342.
[10] G.G. Wildgoose, C.E. Banks, R.G. Compton, Small 2 (2006) 182–193.
[11] Z. liu, X. Lin, J. Lee, W. Zhang, M. Han, L. Gan, Langmuir 18 (2002) 4054–4060.
[12] T. Harada, S. Ikeda, M. Miyazaki, T. Sakata, H. Mori, M. Matsumura, J. Mol. Catal. A: Chem. 268 (2007) 59–64.
[13] A.M. Zhang, J.L. Dong, Q.H. Xu, H.K. Rhee, X.L. Li, Catal. Today 93–95 (2004) 347–352.
[14] W. Chen, X.L. Pan, M.-G. Willinger, D.S. Su, X.H. Bao, J. Am. Chem. Soc. 128 (2006) 3136–3137.
[15] W. Chen, X.L. Pan, M.-G. Willinger, D.S. Su, X.H. Bao, J. Am. Chem. Soc. 129 (2007) 7421–7426.
[16] X.L. Pan, Z.L. Fan, W. Chen, Y.J. Ding, H.Y. Luo, X.H. Bao, Nat. Mater. 6 (2007) 507–511.
[17] W. Chen, Z.L. Fan, X.L. Pan, X.H. Bao, J. Am. Chem. Soc. 130 (2008) 9414–9419.
[18] D. Ugarte, A. Chatelain, W.A. de Heer, Science 274 (1996) 1897–1899.
[19] R.C. Haddon, Science 261 (1993) 1545–1550.
[20] J.C. Charlier, Acc. Chem. Res. 35 (2002) 1063–1069.
[21] J.G. Wang, Y.A. Lv, X.N. Li, M.D. Dong, J. Phys. Chem. C 113 (2009) 890–893.
[22] Y.F. Guo, W.L. Guo, Nanotechnology 17 (2006) 4726–4730.
[23] C.H. Kiang, Carbon 38 (2000) 1699–1701.
[24] K.S.W. Sing, R.T. Williams, Adsorpt. Sci. Technol. 22 (2004) 773–782.
[25] Z.J. Li, Z.W. Pan, S. Dai, Z. Li, Z. Pan, S. Dai, J. Colloid Interf. Sci. 277 (2004) 35–42.
[26] T. Savage, S. Bhattacharya, B. Sadanadan, J. Gaillard, T.M. Tritt, Y.-P. Sun, Y. Wu, S. Naya, R. Car, N. Marzari, P.M. Ajayan, A.M. Rao, J. Phys.: Condens. Matter 15 (2003) 5915–5921.
[27] M. Hulman, H. Kuzmany, Appl. Phys. Lett. 85 (2004) 2068–2070.
[28] J.S. Bendall, A. Ilie, M.E. Welland, J. Sloan, M.L.H. Green, J. Phys. Chem. B 110 (2006) 6569–6573.
[29] S.Y. Ju, F. Papadimitrakopoulos, J. Am. Chem. Soc. 130 (2008) 655–664.
[30] P.A. Gauden, A.P. Terzyk, G. Rychlicki, P. Kowalczyk, K. Lota, E. Raymundo-Pinero, E. Frackowiak, F. Be'guin, Chem. Phys. Lett. 421 (2006) 409–414.
[31] S.Y. Bhide, S. Yashonath, J. Phys. Chem. B 104 (2000) 11977–11986.

[32] P. Kondratyuk, J.T. Yates, Acc. Chem. Res. 40 (2007) 995–1004.
[33] E.E. Santiso, A.M. George, C.H. Turner, M.K. Kostov, K.E. Gubbins, M. Buongiorno Nardelli, M. Sliwinska Bartkowiak, Appl. Surf. Sci. 252 (2005) 766–777.
[34] J. Bian, M. Xiao, S.J. Wang, Y.X. Lu, Y.Z. Meng, Appl. Surf. Sci. 255 (2009) 7188–7196.
[35] E.V. Steen, F.F. Prinsloo, Catal. Today 71 (2002) 327–334.
[36] M.J. Pelletier, Analytical Applications of Raman Spectroscopy, Blackwell Science, Malden, MA, 1999.
[37] B. Burteaux, A. Claye, B.W. Smith, M. Monthioux, D.E. Luzzi, J.E. Fischer, Chem. Phys. Lett. 310 (1999) 21–24.
[38] P. Kondratyuk, Y. Wang, J. Liu, J.K. Johnson, J.T. Yates, J. Phys. Chem. C 111 (2007) 4578–4584.